



Evaluation of nanoscale roughness measurements on a plasma treated SU-8 polymer surface by atomic force microscopy

Ferdinand Walther^a, Wolfgang M. Heckl^{a,b}, Robert W. Stark^{a,*}

^a Center for NanoScience (CeNS) and Department of Earth and Environmental Sciences, Ludwig-Maximilians-Universität München, Theresienstrasse 41, 80333 Munich, Germany

^b Deutsches Museum, Museumsinsel 1, 80356 Munich, Germany

ARTICLE INFO

Article history:

Received 12 February 2008
Received in revised form 20 May 2008
Accepted 21 May 2008
Available online 28 May 2008

PACS:

07.79.Lh
73.61.Ph
46.55._d

Keywords:

AFM
Tip degradation
SU-8
Plasma treatment
Photoresist
Hydrophilisation
Polymer
Intermittent contact

ABSTRACT

A comparison between roughness data obtained with an atomic force microscope (AFM) on different surfaces requires reliable roughness parameters. In order to specify the appropriate parameters for nanoscale roughness measurements, we compared the root mean square (rms) roughness and the relative surface area (sdr) as function of varying scan size, speed and pixel size. By using oxygen plasma (24 kJ) treated SU-8 with an average rms roughness of 2.6 ± 0.5 nm as reference surface, the repeatability of the method was evaluated for dynamic (tapping) and contact mode. The evaluation of AFM images indicated a decrease of the effective tip radius after a few measurements. This degradation of the tip lowers the resolution of the image and can affect roughness measurements.

© 2008 Elsevier B.V. All rights reserved.

1. Introduction

The surface roughness of thin polymer films is an important parameter influencing the functionality of a polymer surface. In order to compare different polymer surfaces or the effect of different surface treatments reliable roughness parameters are needed. In this context, 'reliable' means that the numerical value of the parameter should only weakly depend on the fine-tuning of the characterisation process. Imaging by an atomic force microscope (AFM) provides a convenient characterisation method for nanoscale features on nonconductive surfaces [1,2] although the tips can wear down quickly on hard samples [3]. A comparison between roughness measurements on a glass–ceramic substrate, employing an atomic force microscope (AFM), a stylus, and a non-contact optical profiler highlighted the AFM as instrument with a high spatial resolution, providing the most accurate roughness measurement [4]. For determination of roughness parameters on a

larger scale than a few micrometres, optical profilometers have proved to be valuable tools [5]. In order to compare different surfaces or processes the root-mean-square (rms) roughness parameter is commonly used [6].

A reliable determination of the nano-roughness is important since wetting is strongly affected by the roughness. The role of surface roughness on wetting properties has been extensively studied in order to understand extreme wetting behaviours such as superhydrophilicity or superhydrophobicity. Following Wenzel's ideas, an increased ratio of the actual surface to the geometric surface leads to the enhanced wettability of super-hydrophilic surfaces [7]. A fundamental mechanism of super-hydrophobicity has been assigned to the trapping of air in micro-rough grooves [8]. Superhydrophobic surfaces with a water contact angle greater than 150° can be obtained by combining surface roughness with low surface energy [9,10]. A mixture of micro-rough features in combination with a water repelling surface chemistry leads to the so-called lotus effect. On super hydrophobic surfaces coated by polytetrafluorethene (PTFE), the contact angle increases with the nanoroughness [11]. Apart from the wetting behaviour also frictional properties depend on the surface roughness [6].

* Corresponding author. Tel.: +49 89 2180 4329; fax: +49 89 2180 4334.
E-mail address: stark@lmu.de (R.W. Stark).

Roughness measurements are also employed to control fabrication processes. In order to optimize and monitor process conditions for the fabrication of thin polymer coatings by plasma deposition, roughness measurements are essential tools [12].

In atomic force microscopy, the influence of parameters such as tip roughness, actual surface roughness and humidity on the measured pull-off forces were investigated numerically. The study also showed that roughness data sensitively depend on the tip-surface geometry [13]. An experimental investigation revealed a decrease of the root-mean-square (rms) roughness with increasing tip size (for small scan regions < 500 nm). This effect was attributed to the blunt tips not coming into contact with the lowest areas on the surface. The opposite trend was observed for a scan size of 5 μm , where the rms value increased with the tip size. The inverse effect was proposed to be caused by tip-sample convolution [14]. Additionally, geometric factors of the surface affect also the measured roughness. Depending on the skewness and the standard deviation (rms roughness) of the examined surface, the measured roughness decreases with growing tip radius [15].

By operating the AFM in dynamic mode (tapping or intermittent contact mode) the adhesive contact between tip and sample is broken in each oscillatory cycle. Thus, damage to the sample is reduced with respect to contact mode because lateral and shear forces are smaller on adhesive surfaces. The tip-surface contact time is significantly shortened [16]. Thus the influence of friction and adhesion is reduced. Influences of humidity and surface charging can also affect the imaging process [17,18]. At high relative humidity capillary forces can derogate topography measurements by affecting the non-linear dynamics [17]. Thus, reliable surface roughness experiments should be carried out under moderate humidity. Operating the AFM in the repulsive regime can minimise the effects of surface charges on topography measurements of polymer surfaces [19].

Additionally, reproducible roughness measurements require a well-defined set of operating conditions and parameters such as tip radius, pixel size, scan speed and width. In order to compare results between different sample batches or different laboratories it is important to know the influence of these parameters. Thus, the reliability of roughness parameters has to be monitored as functions of these imaging parameters. In order to verify the influence of various scan parameters and tip wear on the measured roughness on a thin SU-8 film, we conducted a series of AFM measurements. As surface roughness parameters we qualified the root mean square (rms) surface roughness and surface area excess (sdr).

2. Materials and methods

2.1. Thin-film preparation

Silicon (1 0 0) wafers were used as substrates for the SU-8 polymer films. SU-8 is an organic resin solution with the solvent γ -butyrolactone (Microresist Technology GmbH, Berlin, Germany). The fabrication procedure of the polymer film followed the procedure given in the product data sheet. The silicon wafers were cleaned by acetone and ethanol spinning for 30 s at 5000 rpm. For spin coating, 5 ml of SU-8 10 resin solution were applied. The spinning rate was ramped in several steps up to 3000 rpm. After coating, the sample was baked for 2 min on a hot plate at 65 $^{\circ}\text{C}$. Then, the temperature was set to 95 $^{\circ}\text{C}$ for 4 min. After baking, the wafer was cooled slowly to room-temperature. The coated wafers were exposed to UV radiation (Süss MicroTec AG, Garching, Germany) for 2 min. After a post-exposure bake with the same parameters as for the pre-bake, the resist films were developed in

SU-8 XP (Microresist Technology GmbH) for 2 min. Finally, a hard-bake step was carried out at 160 $^{\circ}\text{C}$ for 2 min. The final film thickness was about 10 μm .

For the plasma treatment procedure, we used a microwave-plasma-generator (13.56 MHz, Plasma Technology, Rottenburg, Germany). An oxygen flow of 36 sccm at a pressure of approximately 2×10^{-4} bar was maintained with 0.8 V potential. The reference surface was exposed to oxygen plasma with 50 W energy for 8 min. The sample was stored for 6 months before AFM analysis. The contact angle with water was $65 \pm 4^{\circ}$.

2.2. Atomic force microscopy

Surface roughness measurements were conducted by atomic force microscopy using a Dimension 3100 (Veeco, Santa Barbara, CA) in tapping and in contact mode. Silicon cantilevers with a nominal resonance frequency of 300 kHz, force constant 40 N/m, tip radius < 10 nm (BS-TAP300, BudgetSensors, Sofia, Bulgaria) were used in the dynamic AFM experiments. For contact mode measurements, silicon cantilevers with a nominal resonance frequency of 13 kHz, force constant 0.2 N/m, tip radius < 10 nm (ContAl, BudgetSensors, Sofia, Bulgaria) were used. For each tip, proportional (p_{Gain}) and integral (i_{Gain}) feedback parameters were optimized individually. The feedback parameters were adjusted to provide maximum possible feedback performance while avoiding ringing due to feedback instability. Such a ringing would cause additional noise in the measurement which would lead to an increased apparent surface roughness [20]. The amplitude set-point in dynamic AFM was adjusted in the repulsive regime to approximately 90% in order to minimise tip damage and surface degradation. The relative humidity during the measurements was between 30% and 50%.

The measured surface topography has to represent the shape of surface features. We thus excluded regions of the AFM image from further evaluation, when stripes remained in that region after plane correction and line wise levelling. Some excluded regions also displayed the loss of tip-sample contact. If the shape of the surface features appeared as a self-image of the AFM tip such as repeated triangles or ovals, we discarded the entire image and inserted a new AFM tip. For tapping mode imaging, only reliable images without any artefacts such as streaks or spikes or visible contaminants were evaluated. Thus, we eliminated the effects of severe imaging artefacts, which can easily be detected by an experienced user.

Image processing of the 512×512 pixel comprising data was done using SPIP 4.5 (Image Metrology A/S, Lyngby, Denmark). First, a second-order polynomial plane correction was carried out in order to reduce waviness due to scanner bow and variations of the film thickness. Then a line-wise levelling was performed to reduce a possible line-by-line repetition error. Two roughness parameters will be discussed in the following. The root mean square (rms) surface roughness was calculated using

$$r_{\text{rms}} = \left[\frac{1}{N} \sum_{n=1}^N (z_n - \mu)^2 \right]^{1/2} \quad (1)$$

Here parameter N is the number of data points, z_n height data of the n th point, and μ is the average height. The rms roughness can be regarded as the standard deviation of the height. The ratio between the surface area of the corrugated surface A_r and the projected surface area A_p is the surface area excess defined as

$$r_{\text{sdr}} = \left(\frac{1 - A_r}{A_p} \right) \times 100\% \quad (2)$$

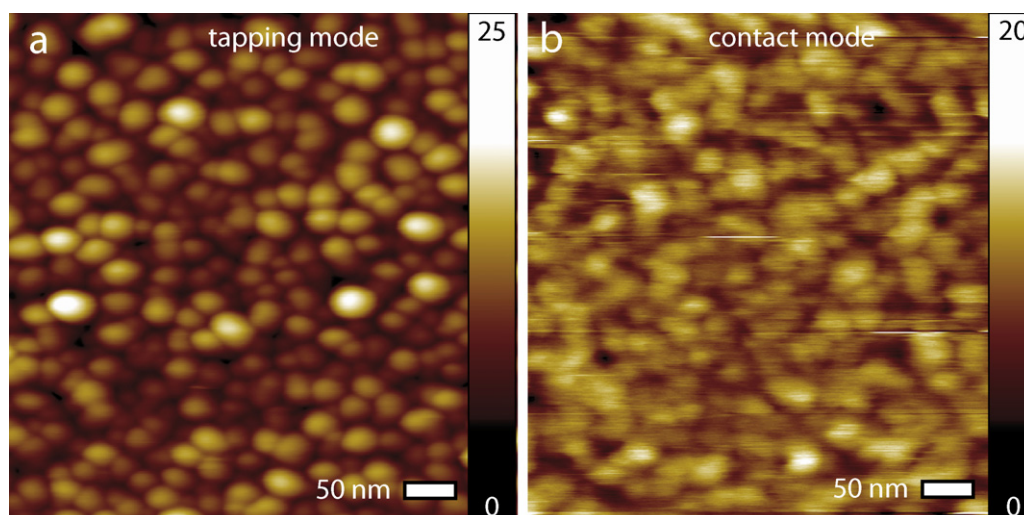


Fig. 1. Topographic AFM images in (a) dynamic and (b) contact mode of oxygen plasma treated SU-8. The surface topography exhibits aggregates of approximately 10–50 nm size and 5–15 nm height which are homogenously distributed across the wafer. Image quality and resolution in dynamic mode are strongly improved.

SPIP 4.5 was used to calculate r_{sdr} . For a completely flat surface, the surface area and the corrugated surface are the same and lead to $r_{sdr} = 0\%$. Physically, this parameter is important as it influences the macroscopic wetting behaviour according to Wenzel's law. The standard variation of the rms and sdr values were obtained by averaging data from several images as indicated. For consistency with previous publications, we used the r_{rms} definition of SPIP 4.5 and earlier. It should be noted, that the definition for r_{rms} has changed since SPIP version 4.6 (see the reference manual). The calculated roughness parameters were collected in an excel sheet and merged together with the feedback parameters p_{Gain} and i_{Gain} . Data evaluation was carried out with Igor 5 (Wavemetrics, Orgeon, USA).

2.3. Scanning electron microscopy

We employed a Zeiss Leo 440i Scanning electron microscope (SEM with an acceleration voltage of 20 kV) at a working distance of 3 mm and a tilt angle of 45°. The polymer sample was sputter coated with gold palladium. AFM tips were characterised without coating.

3. Results and discussion

Fig. 1 displays the oxygen plasma treated SU-8 reference surface imaged both in dynamic and contact mode. Hemispherical aggregates of approximately 10–50 nm width and 5–15 nm height were homogenous distributed across the surface with an rms roughness of 2.3 nm as measured in dynamic mode (Fig. 1(a)). In contact mode, the image resolution is lower and the rms roughness for this image was 1.7 nm (Fig. 1(b)). The image was superposed by streaks due to adhesive tip-surface interactions. We observed that in dynamic mode image resolution and quality were improved as compared to contact mode data (Fig. 1). We thus conclude that for the highly adhesive SU-8 surface (after plasma treatment) dynamic mode imaging provides more reliable roughness data. An SEM micrograph of the plasma treated SU-8 surface (24 kJ plasma dose) allowed for the comparison between the surface topography obtained by AFM (Fig. 1) and images obtained by SEM (Fig. 2a). Similar surface structures appeared in the SEM micrograph and in the AFM image. For a better comparison, one representative AFM image is shown in a three-dimensional plot in Fig. 2(b).

In order to investigate the effect of pixel size, various surface areas with different sizes were imaged. More than seven images for each lateral scan size of 500 nm, 1 μm , 2 μm and 5 μm were obtained while the number of pixels per image was kept at 512×512 pixels. Thus, the surface area of one pixel was varied. The rms values of the different images were close to the average of 2.6 nm with a standard deviation of ± 0.03 nm (Fig. 3(a)). Thus, within the investigated range, the rms roughness did not depend on the pixel size. In contrast, the excess surface area (sdr) decreased from $8.7 \pm 3.9\%$ for small pixels (area 0.96 nm^2) to $2.9 \pm 0.8\%$ for large pixels with 95 nm^2 area. The sdr value was reduced to one-third by increasing pixel size. The mean sdr roughness was $\text{sdr} = 5.9 \pm 2.8\%$.

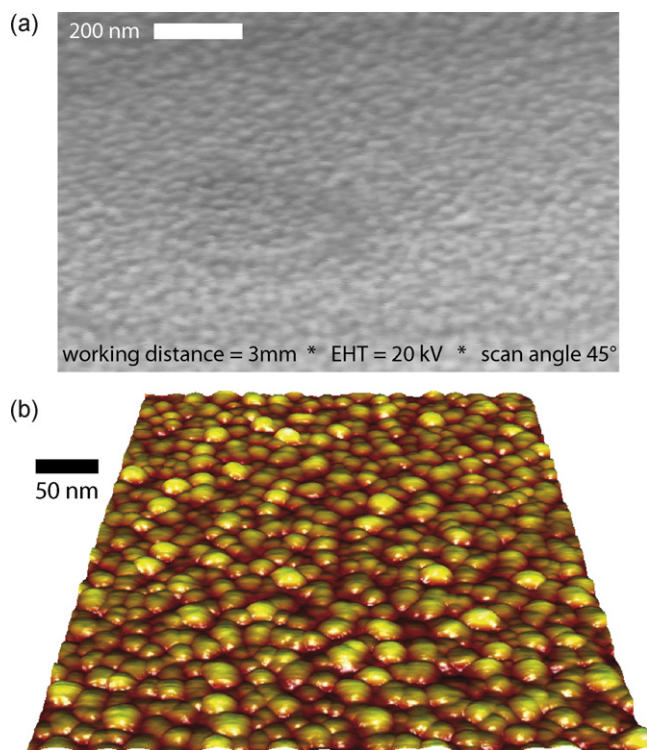


Fig. 2. (a) SEM-micrograph of SU-8 after oxygen plasma treatment (24 kJ). (b) Topographic AFM data (500 nm \times 500 nm) of the same surface in a 3D representation (rms = 2.3 nm).

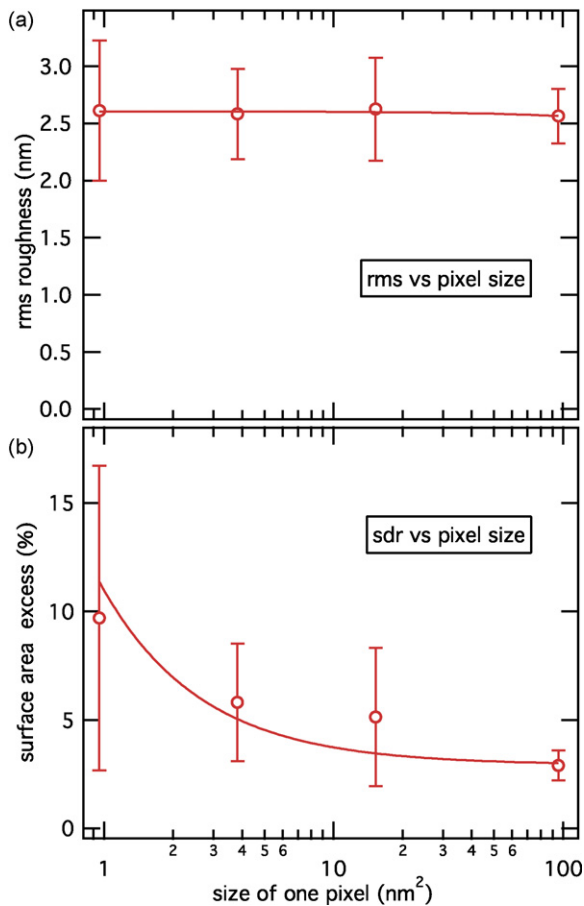


Fig. 3. The (a) rms and (b) sdr roughness parameters as functions of the pixel size. 512 pixels were measured across a scan range of 500 nm, 1 μm , 2 μm and 5 μm , resulting in the area of one pixel with (9 nm², 19 nm², 39 nm², 97 nm²). Data in (a) was fitted by linear regression and in (b) with a 1/x-function. Both functions serve as a guide for the eye and do not imply a physical model.

For a reliable comparison, the pixel area should be the same to avoid biasing of the results by a quantisation artefact (Fig. 3(b)).

The influence of the scan speed on the surface roughness is visualized in Fig. 4. The feedback parameters (Fig. 4(a)) were optimised for each tip and scan speed individually, in order to achieve the best possible surface tracking (smallest possible error signal). This optimisation leads to the scatter of the respective i_{Gain} values between 0.02 and 0.31. Imaging was carried out at various scan speeds (0.5, 1.0, 1.3, 2.0, 2.5, 5.0 $\mu\text{m/s}$), including at least seven images per speed. For the data point at a scan speed of 5 $\mu\text{m/s}$ we consolidated all data from 4.2 to 6.1 $\mu\text{m/s}$. In the velocity range from 0.6 to 5.0 $\mu\text{m/s}$, the rms values have an average of $\text{rms} = 2.6 \pm 0.2 \text{ nm}$ (Fig. 4(a)). The rms values scattered between 1.9 nm (at 5 $\mu\text{m/s}$) and 3.9 nm (at 1.4 $\mu\text{m/s}$). The average surface area excess was $\text{sdr} = 7.7 \pm 1.7\%$ (Fig. 4(b)). In contrast to the moderate variation of the rms roughness, the sdr roughness scatters between 1.7% (at 5 $\mu\text{m/s}$) and 27.5% (at 2 $\mu\text{m/s}$). The sdr roughness is sensitive to variation of the scan speed.

In both previous experiments, varying either pixel size or the scan speed, the standard deviation of the sdr roughness as measured in several images exceeds that one for the rms roughness. No dependency between scan speed and rms roughness could be identified. Nevertheless, measuring bigger scan sizes appeared to wear the AFM tip faster than smaller scan sizes. In contrast, the relative surface area exhibits a stronger variation with a tendency to decreasing sdr values for higher scan speeds. This

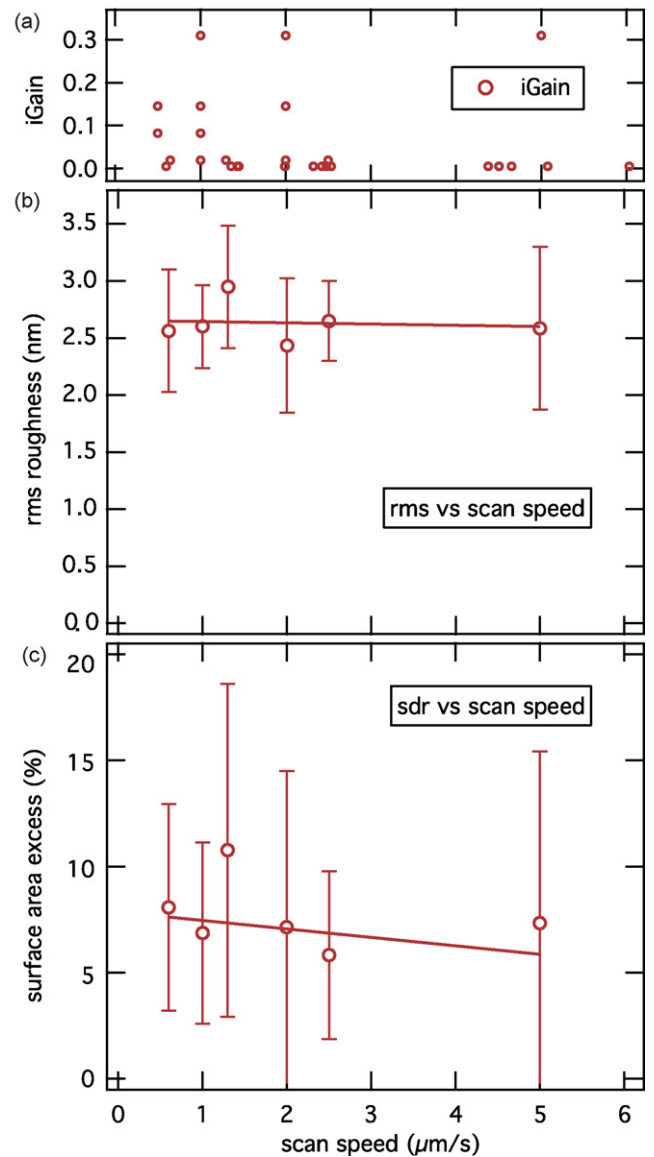


Fig. 4. Roughness parameters as functions of the scan speed (0.6, 1.0, 1.3, 2.0, 2.5, 5.0 $\mu\text{m/s}$). (a) The respective feedback parameters, (b) rms and (c) sdr roughness. The lines indicate a linear regression. The average rms value is $2.6 \pm 0.2 \text{ nm}$ and the sdr value $7.7 \pm 1.7 \text{ nm}$.

dependency of the sdr roughness on scan speed can be attributed to the feedback regulation mechanism. By increasing the scan speed the efficiency of the feedback is reduced since the gains cannot be increased beyond a certain level (onset of instability of the closed loop). The controller thus acts as a low-pass filter for the control signal. Since the control signal directly corresponds to the topography signal, the measured topography is low-pass filtered and sharp surface features such as peaks and valleys appear broader. This smoothing of the surface topography mainly affects the sdr value whereas the rms value is less sensitive to this filtering effect.

Another important factor is wear down of the tip in repeated measurements. In Fig. 5(a), the rms roughness is plotted versus the consecutive number of the measurement, using dynamic mode. A vertical line indicates a tip exchange. The tip was exchanged, when typical tip artefacts such as tip self-imaging or streaks occurred. Each measurement was carried out on another region of the sample to avoid wear down of the specimen. For these topography

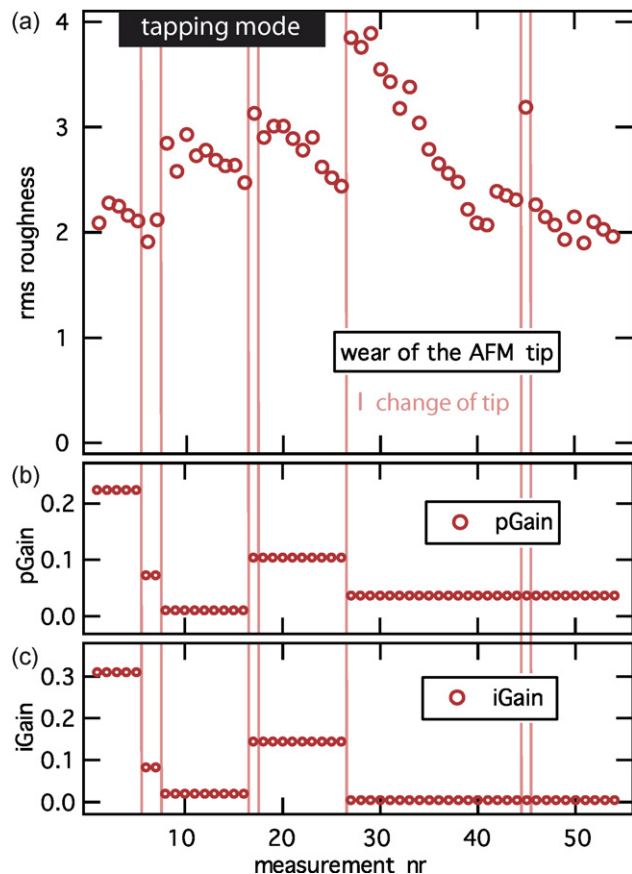


Fig. 5. (a) Consecutively measured rms roughness values obtained on the same SU-8 surface in dynamic mode. Tip changes are indicated by vertical lines. The (b) i_{Gain} and (c) p_{Gain} settings of the AFM were optimised for each tip individually.

data, the average roughness of the entire data set is $\text{rms}_{\text{tap}} = 2.6 \pm 0.5$ nm. The smallest measured roughness was 1.9 nm and the largest 3.9 nm. Fig. 5(b and c) indicates the feedback parameters i_{Gain} and p_{Gain} . The feedback parameters were kept constant for each tip, in order to eliminate their influence on the roughness parameters. During the use of one AFM tip, the measured rms roughness decreased from image to image. Within 5–10 images

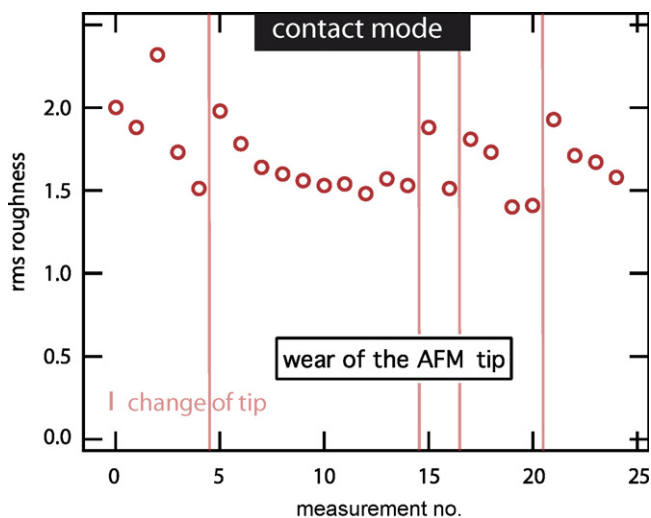


Fig. 6. Consecutively measured rms roughness values obtained on the same SU-8 surface in contact mode. Tip changes are indicated by vertical lines.

made with a single tip, the rms roughness decreased by typically 0.5 nm. This means, that the measured roughness as determined by a single AFM tip decreased by 20% after a few good AFM images. Imaging bigger scan sizes yield to a faster decrease of the measured roughness.

A similar experiment was carried out in contact mode. Fig. 6 represents the rms roughness as function of the measurement number as obtained in contact mode. The average roughness of the entire data set in contact mode is $\text{rms}_{\text{cont}} = 1.7 \pm 0.2$ nm. The smallest measured roughness in contact mode was 1.4 nm and the largest 2.3 nm rms roughness values obtained in contact mode were in average more than 35% smaller than in tapping mode—for the same surface.

To check the degree of tip degradation, we imaged a used AFM tip (BS-TAP300) by SEM (Fig. 7). This tip was employed for measuring more than 20 images on SU-8 with a cross section of various scan sizes and speeds. The AFM image quality obtained with this tip was reduced and the surface mapping showed artefacts and stripes. rms roughness data obtained with this tip had decreased to less than 50% of the initial values. Fig. 7(b) indicates that the tip apex is degenerated and polymer material was attached. From the SEM data the tip radius was estimated to approximately 40 nm.

Thus, we attribute the decreasing surface roughness observed in all consecutive AFM measurements to an increase of tip radius. This includes a wear down of tip and polymer material adhering to the tip. A variation of the tip radius out of the box and individual fine tuning of the feedback parameters yield to initial rms measurements in a range from 2 to 4 nm. With bigger scan sizes

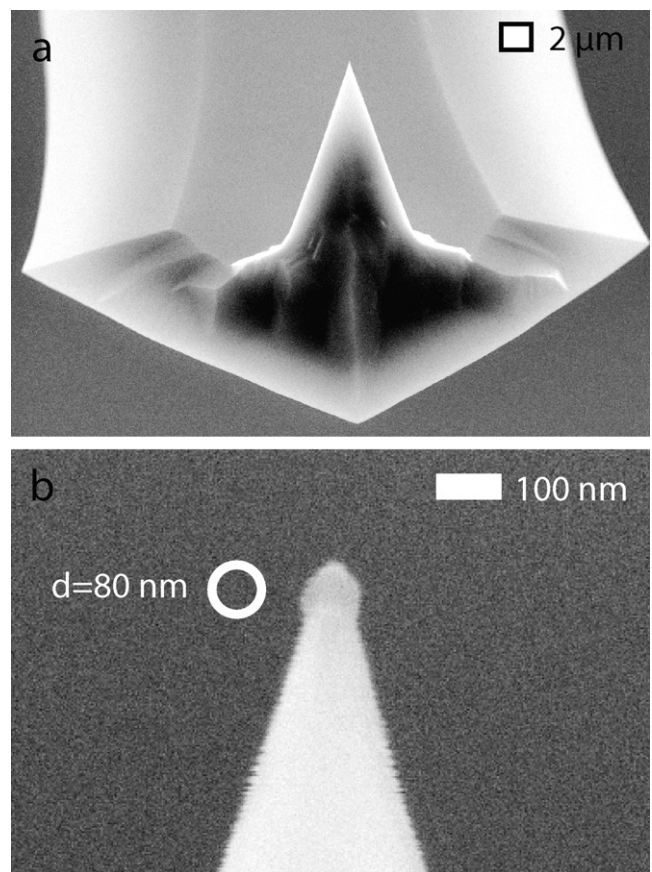


Fig. 7. (a) SEM-micrograph of an AFM tip after dynamic mode imaging (SEM: working distance 3 mm, EHT 20 kV). (b) Detail of the tip apex. The tip radius is approximately 40 nm.

the tip wear is accelerated. Together, these effects lead to a decreased imaging resolution and therefore to a reduced rms roughness.

4. Conclusions

The surface roughness of a SU-8 surface was evaluated by AFM after plasma treatment. The measurements highlighted the variations of roughness parameters as obtained by AFM. A focus was on the influence of the measurement parameters and the variability from tip-to-tip on rms and sdr values. Consecutive imaging with one tip at different spots on the surface led to a decrease of rms roughness by 20% within 5–10 images. Thus, besides the variation from tip-to-tip out of the box, tip degradation during imaging can lead to a significant error within a few images. Within the experiment, the tip alters by wear down of tip material or by attachment of polymer material from the surface. Both effects lead to an increase of the tip radius. We therefore suggest using a new tip after a few of images in order to obtain reliable roughness parameters. A reliable determination of the surface roughness of a certain sample also requires statistic averaging over several AFM tips. In order to reduce the influence of adhesive forces between tip and surface on the measured roughness values, imaging in dynamic mode is advantageous. Additionally, one has to keep in mind that the selected roughness parameter can depend on pixel size, scan width and speed. The rms roughness was robust against variations of these parameters within the investigated parameter range. As long as scan speed and feedback parameters are selected thus that the AFM tip can fully trace the surface topography, the rms evaluation is a reliable parameter to compare surface roughnesses obtained on different specimens. In contrast, the relative surface area (sdr) strongly depended on the scan parameters. For this parameter, a comparison of different surfaces is only reliable, if the scan parameters are not changed. Concluding,

we suggest the rms roughness as a useful parameter for the comparison of the nanoroughness of polymer surfaces.

Acknowledgements

We thank Marc Hennemeyer, Ayhan Yurtsever and Alexander Gigler (LMU) for fruitful discussions and Klaus Macknapp (Deutsches Museum) for SEM imaging. We gratefully acknowledge financial support by the German Federal Ministry of Education and Research (BMBF) grant “Nanofutur” 03N8706.

References

- [1] R. Garcia, R. Perez, *Surface Science Reports* 47 (2002) 197–301.
- [2] F. Walther, P. Davydovskaya, S. Zucher, M. Kaiser, H. Herberg, A.M. Gigler, R.W. Stark, *Journal of Micromechanics and Microengineering* 17 (2007) 524–531.
- [3] P. Bakucz, A. Yacoot, T. Dziomba, L. Koenders, R. Krüger-Sehm, *Measurement Science and Technology* 19 (2008) 065101.
- [4] C.Y. Poon, B. Bhushan, *Wear* 190 (1995) 76–88.
- [5] T.P. Kunzler, T. Drobek, C.M. Sprecher, M. Schuler, N.D. Spencer, *Applied Surface Science* 253 (2006) 2148–2153.
- [6] B. Bhushan, *Wear* 259 (2005) 1507–1531.
- [7] R.N. Wenzel, *Industrial and Engineering Chemistry* 28 (1936) 988–994.
- [8] A.B.D. Cassie, S. Baxter, *Transactions of the Faraday Society* 40 (1944) 0546–0550.
- [9] L. Guo, W. Yuan, J. Li, Z. Zhang, Z. Xie, *Applied Surface Science* 254 (2008) 2158–2161.
- [10] Q. Wang, B. Zhang, M. Qu, Z. Junyan, D. He, *Applied Surface Science* 254 (2008) 2009–2012.
- [11] J.D. Miller, S. Veeramasuneni, J. Drelich, M.R. Yalamanchili, G. Yamauchi, *Polymer Engineering and Science* 36 (1996) 1849–1855.
- [12] G.W. Collins, S.A. Letts, E.M. Fearon, R.L. McEachern, T.P. Bernat, *Physical Review Letters* 73 (1994) 708–711.
- [13] J. Jang, J. Sung, G.C. Schatz, *Journal of Physical Chemistry C* 111 (2007) 4648–4654.
- [14] D.L. Sedin, K.L. Rowlen, *Applied Surface Science* 182 (2001) 40–48.
- [15] Y.H. Chen, W.H. Huang, *Measurement Science & Technology* 15 (2004) 2005–2010.
- [16] J. Tamayo, R. Garcia, *Langmuir* 12 (1996) 4430–4435.
- [17] L. Zitzler, S. Herminghaus, F. Mugele, *Physical Review B* 66 (2002) 155436.
- [18] D. Ziegler, J. Rychen, N. Naujoks, A. Stemmer, *Nanotechnology* 18 (2007) 225505.
- [19] R.W. Stark, N. Naujoks, A. Stemmer, *Nanotechnology* 18 (2007) 065502.
- [20] D. Tranchida, S. Piccarolo, R.A.C. Deblieck, *Measurement Science & Technology* 17 (2006) 2630–2636.